nature physics

ARTICLES

https://doi.org/10.1038/s41567-021-01445-3

Check for updates

General construction and topological classification of crystalline flat bands

Dumitru Călugăru[1,7], Aaron Chew[1,7], Luis Elcoro[2,7], Yuanfeng Xu[1,3], Nicolas Regnault[1,4], Zhi-Da Song[1] and B. Andrei Bernevig[1,5,6] ✉

Exotic phases of matter can emerge from the interplay between strong electron interactions and non-trivial topology. Materials that have non-dispersing bands in their electronic band structure, such as twisted bilayer graphene, are prime candidates for strongly interacting physics. However, existing theoretical models for obtaining these 'flat bands' in crystals are often too restrictive for experimental realizations. Here we present a generic theoretical technique for constructing perfectly flat bands from bipartite crystalline lattices. Our prescription encapsulates and generalizes the various flat-band models in the literature and is applicable to systems with any orbital content, with or without spin–orbit coupling. Using topological quantum chemistry, we build a complete topological classification in terms of symmetry eigenvalues of all the gapped and gapless flat bands. We also derive criteria for the existence of symmetry-protected band touching points between the flat and dispersive bands, and identify the gapped flat bands as prime candidates for fragile topological phases. Finally, we show that the set of all perfectly flat bands is finitely generated and construct the corresponding bases for all 1,651 Shubnikov space groups.

Under special conditions, translation-invariant systems harbour perfectly flat bands, that is, spectral bands with momentum-independent energy. This extensive single-particle degeneracy of electron states leads to a completely non-perturbative effect of arbitrary levels of interactions or disorder, making flat-band systems prime candidates for strongly correlated phases of matter. Perhaps the most exciting recent developments in this direction concern twisted bilayer graphene, where the almost flat bands[1] have been linked to a plethora of magnetic and superconducting phases[2,3].

Furthermore, consequent theoretical studies have also highlighted the importance of the non-trivial topology of the flat bands[4–7]. For example, Ginzburg–Landau theory predicts a vanishing superfluid weight for perfectly flat bands. However, a topologically non-trivial flat band has additional band-geometric contributions to the superfluid weight and can thus show superconductive behaviour[7].

Flat bands arising from wavefunction interference are a very rich playground for physical phenomena. In crystalline materials, the rich physics of interacting flat-band systems predates the advent of twisted bilayer graphene, with theoretical proposals of flat bands playing host to Hubbard ferromagnetism[8,9], Wigner crystallization[10], supersolid formation[11] or Anderson transition[12,13]. However, the well-known theoretical constructions of flat bands, such as the line-graph prescription[8,9,14–16], are often restricted to toy models comprising *s* orbitals and non-spin–orbit-coupled Hamiltonians with various geometric constraints, such as nearest-neighbour hoppings with the same sign. These simplifications have hindered the discovery of real-life crystalline materials with flat bands[17–19], which are usually obtained in optical lattices[20] or superconducting circuits[21].

In this paper, we introduce a generic technique for constructing perfectly flat bands in bipartite crystalline lattices (BCLs), where a lattice is divided into two sublattices with unequal numbers of orbitals. The BCL construction can be applied to any type of orbitals, with or without spin–orbit coupling, and in any of the 1,651 Shubnikov space groups, including the space groups with or without time-reversal symmetry and the magnetic space groups. Our prescription also encapsulates and generalizes the line-graph[8,9,14–16,21–24] and split-graph[23–25] formulations, as well as many of the models presented in literature[5,10,22,23,26–33]. Additionally, our formalism correctly explains the origin of flat bands in myriad real-life materials, as highlighted in an accompanying paper[34]. Applying magnetic topological quantum chemistry (MTQC)[35,36] and related theories[37–39] to our construction yields our main result: flat bands can be understood as formal differences of band representations. This enables us to derive universal criteria for the existence of symmetry-protected band touching points between the flat and dispersive bands, which were previously only explained in an ad hoc manner[22,40]. Moreover, gapped flat bands can realize any commensurate difference of band representations, and thus are prime candidates for fragile topological phases[23,35,41–44]. Finally, we show that the set of all perfectly flat bands is finitely generated and construct the corresponding bases in all Shubnikov space groups.

Model

We first outline the BCL construction (Supplementary Section IA). A BCL is a translation-invariant fermionic lattice partitioned into two different sublattices, L and $\tilde{L}$. We assume that each sublattice individually respects all the symmetries of the BCL's Shubnikov space group. For each unit cell $\mathbf{R}$, we define fermionic annihilation operators $\hat{a}_{\mathbf{R},i}$ ($\hat{b}_{\mathbf{R},i}$) corresponding to each orbital i from sublattice L ($\tilde{L}$). For spinful fermions, different spin states have different indices i. Within each sublattice L and $\tilde{L}$, we place N_L and $N_{\tilde{L}}$ orbitals per unit cell, respectively, and introduce a unitary chiral operator

[1]Department of Physics, Princeton University, Princeton, NJ, USA. [2]Department of Condensed Matter Physics, University of the Basque Country UPV/EHU, Bilbao, Spain. [3]Max Planck Institute of Microstructure Physics, Halle, Germany. [4]Laboratoire de Physique de l'École normale supérieure, ENS, Université PSL, CNRS, Sorbonne Université, Université Paris-Diderot, Paris, France. [5]Donostia International Physics Center, Donostia-San Sebastian, Spain. [6]IKERBASQUE, Basque Foundation for Science, Bilbao, Spain. [7]These authors contributed equally: Dumitru Călugăru, Aaron Chew and Luis Elcoro. ✉e-mail: bernevig@princeton.edu

C acting differently on the two sublattices: $C\hat{a}^\dagger_{\mathbf{R},i}C^{-1} = \hat{a}^\dagger_{\mathbf{R},i}$ and $C\hat{b}^\dagger_{\mathbf{R},i}C^{-1} = -\hat{b}^\dagger_{\mathbf{R},i}$. We first consider quadratic Hamiltonians $\mathcal{H}$ with anti-commuting chiral symmetry (that is, $\{C, \mathcal{H}\} = 0$) and later relax this constraint. Defining momentum space operators $\hat{c}_{\mathbf{k},i} = \frac{1}{\sqrt{N}}\sum_{\mathbf{R}} \hat{c}_{\mathbf{R},i}e^{i\mathbf{k}\cdot(\mathbf{R}+\mathbf{r}_i)}$, where $\mathbf{r}_i$ denotes the position of the ith orbital relative to the unit cell origin and $\hat{c} = \hat{a}, \hat{b}$ for the two sublattices, the Hamiltonian (which includes only inter-sublattice hopping) can be written as $\mathcal{H} = \sum_{\mathbf{k}} \hat{\Psi}^\dagger_{\mathbf{k}} H_{\mathbf{k}} \hat{\Psi}_{\mathbf{k}}$, where the first-quantized Hamiltonian matrix is

$$H_{\mathbf{k}} = \begin{pmatrix} & S_{\mathbf{k}} \\ S^\dagger_{\mathbf{k}} & \end{pmatrix} \tag{1}$$

and $\hat{\Psi}^{\mathrm{T}}_{\mathbf{k}} = \left(\hat{a}_{\mathbf{k},1}, \ldots, \hat{a}_{\mathbf{k},N_L}, \hat{b}_{\mathbf{k},1}, \ldots, \hat{b}_{\mathbf{k},N_{\tilde{L}}}\right)$ is an $(N_L + N_{\tilde{L}})$-dimensional spinor. In equation (1), C forbids any intra-sublattice hopping terms, whilst $S_{\mathbf{k}}$ denotes the $N_L \times N_{\tilde{L}}$ hopping matrix between different sublattices[25]. Its rank $r_{\mathbf{k}}$ is bounded by its smaller dimension. Taking $N_L > N_{\tilde{L}}$, it follows (Supplementary Section IB) that $H_{\mathbf{k}}$ contains at least $N_L - N_{\tilde{L}}$ zero modes for all $\mathbf{k}$, yielding $N_L - N_{\tilde{L}}$ perfectly flat bands, and $2N_{\tilde{L}}$ dispersive bands coming in pairs related by chiral symmetry. Generically, $S_{\mathbf{k}}$ has maximal rank $r_{\mathbf{k}}$ for all $\mathbf{k}$, except at band touching points between the flat and the dispersive bands.

The Hamiltonian $H_{\mathbf{k}}$ is diagonalized using the singular value decomposition $S_{\mathbf{k}} = W_{\mathbf{k}}\Sigma_{\mathbf{k}}V^\dagger_{\mathbf{k}}$, where $W_{\mathbf{k}}$ ($V_{\mathbf{k}}$) denotes an $N_L \times N_L$ ($N_{\tilde{L}} \times N_{\tilde{L}}$) unitary matrix, whilst $\Sigma_{\mathbf{k}}$ is a diagonal $N_L \times N_{\tilde{L}}$ matrix of singular values (listed in descending order). We define $\psi_{\mathbf{k},\alpha}$ ($\phi_{\mathbf{k},\alpha}$) to be the vector formed by the αth column of $V_{\mathbf{k}}$ ($W_{\mathbf{k}}$). For each $\alpha \leq r_{\mathbf{k}}$, the dispersive bands' eigenvectors are

$$\Psi^{\pm}_{\mathbf{k},\alpha} = \frac{1}{\sqrt{2}}\begin{pmatrix} \pm\phi_{\mathbf{k},\alpha} \\ \psi_{\mathbf{k},\alpha} \end{pmatrix}, \tag{2}$$

with energies $\pm\epsilon_{\mathbf{k},\alpha}$, where $\epsilon_{\mathbf{k},\alpha}$ is the αth singular value of $S_{\mathbf{k}}$ (that is, the αth nonzero diagonal entry of $\Sigma_{\mathbf{k}}$). The zero modes of $H_{\mathbf{k}}$ are $\Psi^{+\mathrm{T}}_{\mathbf{k},\alpha} = \left(\phi^{\mathrm{T}}_{\mathbf{k},\alpha}, 0\right)$ for $r_{\mathbf{k}} < \alpha \leq N_L$ and $\Psi^{-\mathrm{T}}_{\mathbf{k},\alpha} = \left(0, \psi^{\mathrm{T}}_{\mathbf{k},\alpha}\right)$ for $r_{\mathbf{k}} < \alpha \leq N_{\tilde{L}}$, with $S_{\mathbf{k}}\psi_{\mathbf{k},\alpha} = 0$ and $S^\dagger_{\mathbf{k},\boldsymbol{\alpha}}\phi_{\mathbf{k},\alpha} = 0$, respectively. These include both the flat-band eigenstates (for which $S^\dagger_{\mathbf{k}}\phi_{\mathbf{k},\alpha} = 0$ for all $\mathbf{k}$) and the zero modes of the dispersive bands at the band touching points (where $r_{\mathbf{k}} < N_{\tilde{L}}$).

It is instructive to consider 'integrating' out the degrees of freedom on the smaller sublattice $\tilde{L}$. This is equivalent to adding a large chemical potential term for the orbitals in sublattice $\tilde{L}$ and then including their effects on sublattice L using degenerate second-order perturbation theory (Supplementary Section IC). Up to multiplicative factors and constant offsets, the resulting effective Hamiltonian is $T_{\mathbf{k}} = S_{\mathbf{k}}S^\dagger_{\mathbf{k}}$. The eigenvectors of $T_{\mathbf{k}}$ are $\phi_{\mathbf{k},\alpha}$ ($1 \leq \alpha \leq N_L$) and thus include the flat-band modes of the original BCL (being in the kernel of $S^\dagger_{\mathbf{k}}$, they are also zero modes of $T_{\mathbf{k}}$). Alternatively, one may integrate the other sublattice yielding the Hamiltonian $\tilde{T}_{\mathbf{k}} = S^\dagger_{\mathbf{k}}S_{\mathbf{k}}$, whose eigenstates $\psi_{\mathbf{k},\alpha}$ ($1 \leq \alpha \leq N_{\tilde{L}}$) do not include the flat-band modes, but that possesses the same nonzero eigenvalues as $T_{\mathbf{k}}$: $\epsilon^2_{\mathbf{k},\alpha}$ ($1 \leq \alpha \leq r_{\mathbf{k}}$). There is also a direct mapping between the nonzero eigenstates of the two Hamiltonians: $\phi_{\mathbf{k},\alpha} = \frac{1}{\epsilon_{\mathbf{k},\alpha}}S_{\mathbf{k}}\psi_{\mathbf{k},\alpha}$. Because $H_{\mathbf{k}}$ and $T_{\mathbf{k}}$ possess identical flat-band wavefunctions and share the same Shubnikov space group, both yield the same flat-band topology. Additionally, this formal integration procedure resembles the construction of a line-graph Hamiltonian ($T_{\mathbf{k}}$) from a Hamiltonian defined on a 'root' Euclidean graph ($\tilde{T}_{\mathbf{k}}$) using the incidence matrix of the latter ($S_{\mathbf{k}}$) (ref. [8]). Unlike the line-graph construction, in the BCL construction, $S_{\mathbf{k}}$ can denote any type of inter-sublattice hopping matrix between any orbitals (with or without spin–orbit coupling) and is not restricted to binary incidence matrices in spinless systems of s orbitals. We present several examples, including an analysis of flat bands of the real material $Ca_2Ta_2O_7$ (ref. [34]), in Supplementary Section II.

The chiral BCL Hamiltonian $\mathcal{H}$ can be generalized by including generic intra-sublattice hopping terms within the $\tilde{L}$ sublattice, which break the chiral symmetry without perturbing the flat bands. To see this, consider the Hamiltonian

$$H_{\mathbf{k}} = \begin{pmatrix} A_{\mathbf{k}} & S_{\mathbf{k}} \\ S^\dagger_{\mathbf{k}} & B_{\mathbf{k}} \end{pmatrix}, \tag{3}$$

where $A_{\mathbf{k}}$ ($B_{\mathbf{k}}$) is an $N_L \times N_L$ ($N_{\tilde{L}} \times N_{\tilde{L}}$) Hermitian matrix denoting the intra-sublattice hopping inside the L ($\tilde{L}$) sublattice. We assume that $A_{\mathbf{k}}$ has a momentum-independent eigenvalue a with degeneracy n_a. If $N_{\tilde{L}} < n_a \leq N_L$, then the Hamiltonian in equation (3) has at least $n_a - N_{\tilde{L}}$ flat bands of energy a irrespective of $B_{\mathbf{k}}$ (Supplementary Section ID). The simplest case is for $A_{\mathbf{k}}$ to be proportional to the identity matrix (that is, $A_{\mathbf{k}} = a\mathbb{1}$), with arbitrary $B_{\mathbf{k}}$, a construction which we term a generalized BCL. A more general possibility occurs when $A_{\mathbf{k}}$ itself is a BCL Hamiltonian with n_a perfectly flat bands. Hence $A_{\mathbf{k}}$ is a generalized BCL Hamiltonian comprising sublattices L' and $\tilde{L}'$ with $n_a = N_{L'} - N_{\tilde{L}'}$. However, redefining $\tilde{L} \leftarrow \tilde{L}'$ and $L \leftarrow L \oplus L'$ brings the Hamiltonian back into the form of equation (3) with $A_{\mathbf{k}}$ proportional to identity (Supplementary Section ID). We henceforth consider $A_{\mathbf{k}} = a\mathbb{1}$. Moreover, because they are in the kernel of $S^\dagger_{\mathbf{k}}$ and have support only on the L sublattice, the chiral BCL flat-band eigenstates $\Psi^{+}_{\mathbf{k},\alpha}$ (and corresponding band touching points) for $r_{\mathbf{k}} < \alpha \leq N_L$ will remain eigenvectors of $H_{\mathbf{k}}$, but with eigenvalue a. The corresponding flat-band and band touching point wavefunctions are unaffected by the introduction of the intra-sublattice hopping matrices. However, the band touching points corresponding to $\Psi^{-}_{\mathbf{k},\alpha}$ for $r_{\mathbf{k}} < \alpha \leq N_{\tilde{L}}$ will generically be gapped. This implies that the topological properties of the flat bands and their band touching points in a generalized BCL can be inferred from the zero modes of $T_{\mathbf{k}} = S_{\mathbf{k}}S^\dagger_{\mathbf{k}}$. The zero modes of $\tilde{T}_{\mathbf{k}} = S^\dagger_{\mathbf{k}}S_{\mathbf{k}}$ will not correspond to band touching points in the generalized BCL Hamiltonian from equation (3).

Symmetries in a BCL. MTQC diagnoses the topology of a band via its (co)irreps at high-symmetry momenta[35,36,38,39]. We assume that the BCL Hamiltonian from equation (1), as well as each of its two sublattices individually, are invariant under a certain Shubnikov space group $\mathcal{G}$ (in principle, each sublattice might be invariant under a supergroup of $\mathcal{G}$, which will not be considered in this paper). At a high-symmetry momentum $\mathbf{K}$, the inter-sublattice hopping matrix is invariant under any transformation belonging to $\mathcal{G}_{\mathbf{K}}$, the little group of $\mathbf{K}$ (that is, the subgroup of $\mathcal{G}$ that leaves $\mathbf{K}$ invariant, up to reciprocal lattice vectors). The action of the symmetries in $\mathcal{G}_{\mathbf{K}}$ on the eigenstates of $T_{\mathbf{K}}$ and $\tilde{T}_{\mathbf{K}}$ gives rise to (co)irreps of $\mathcal{G}_{\mathbf{K}}$. At the same time, the eigenvectors of $T_{\mathbf{K}}$ and $\tilde{T}_{\mathbf{K}}$ with identical nonzero energies are mapped to one another by the symmetry-invariant matrix $S_{\mathbf{K}}$, and thus furnish identical (co)irreps (Methods). Therefore, the dispersive bands of $T_{\mathbf{k}}$ and $\tilde{T}_{\mathbf{k}}$ not only are identical in energies but also share identical (co)irreps at high-symmetry momenta. The only exceptions are the zero modes of the two effective Hamiltonians for which there is no direct mapping between the eigenstates. An indirect mapping between their (co)irreps will be derived below.

Flat-band (co)irreps. Since $T_{\mathbf{k}}$ is defined on the L sublattice, the band representations corresponding to all the bands (including the flat bands) of $T_{\mathbf{k}}$ ($\mathcal{BR}_L$) are the sum of all elementary band representations induced from the orbitals of the L sublattice. Similarly, the band representations of all the bands of $\tilde{T}_{\mathbf{k}}$ ($\mathcal{BR}_{\tilde{L}}$) are the sum of all elementary band representations induced from the orbitals of $\tilde{L}$. Moreover, the dispersive bands of $T_{\mathbf{k}}$ and $\tilde{T}_{\mathbf{k}}$ share the same

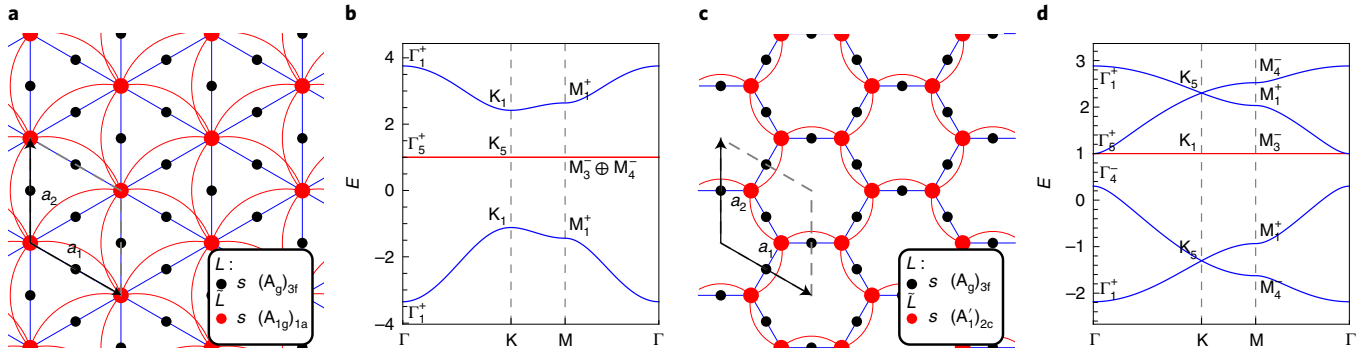

Fig. 1 | Examples of flat-band constructions in generalized BCLs. The structure of two BCLs defined on the hexagonal lattice is shown in **a** and **c**. In both cases, we place *s* orbitals at the 3f position within sublattice L (black dots), whilst $\tilde{L}$ contains *s* orbitals at the 1a (**a**) and 2c (**c**) position (red dots). Red and blue lines respectively denote intra-sublattice hopping with amplitude t_2 within $\tilde{L}$ and inter-sublattice hopping with amplitude t_1. There is a degenerate on-site energy term ϵ on sublattice L. Corresponding band structures at $t_1 = -1$ (**b**) and $t_2 = -0.1$ (**d**), together with corresponding (co)irreps[35,36,45–47].

(co)irreps at high-symmetry momentum points, except for the zero modes in $\tilde{T}_{\mathbf{k}}$ (or, equivalently, the band touching points with the flat bands in $T_{\mathbf{k}}$). As such, the (co)irreps of the perfectly flat bands in $T_{\mathbf{k}}$ (denoted by $\mathcal{B}_{\mathrm{FB}}$), which are identical to the flat bands of the generalized BCL Hamiltonian from equation (3), are independent of the inter-sublattice hopping matrix $S_{\mathbf{k}}$ and must be given by those (co) irreps of $\mathcal{BR}_L$ which are not in $\mathcal{BR}_{\tilde{L}}$:

$$\mathcal{B}_{\mathrm{FB}} = \mathcal{BR}_L \boxminus \mathcal{BR}_{\tilde{L}}. \tag{4}$$

Formally, in equation (4), we introduced an identity element $\emptyset$ for the direct sum operation of (co)irreps ($\oplus$) and an 'inverse' $\boxminus\Xi$ to each (co)irrep Ξ, such that $\Xi \oplus (\boxminus\Xi) = \emptyset$. When evaluating differences ($\boxminus$) of (co)irreps, we will encounter expressions such as $(\Gamma_2 \oplus \Gamma_3) \boxminus (\Gamma_1 \oplus \Gamma_3) = \Gamma_2 \boxminus \Gamma_1$ that cannot be simplified further to (co)representation. These differences are instrumental in understanding the band touching points between the flat and the dispersive bands arising in a generalized BCL (Supplementary Section IF).

Band touching points. First, when $\mathcal{BR}_{\tilde{L}}$ is a subset of $\mathcal{BR}_L$ at a given momentum point $\mathbf{K}$, such that equation (4) produces a bona fide (co)representation at $\mathbf{K}$, there can be no locally stable band touching points between the flat and dispersive bands of the BCL protected by crystalline symmetries (Methods). Here, we define a locally stable band touching point as a band touching point that can neither be gapped completely nor have its location in momentum space changed by any symmetry-preserving perturbation to the $S_{\mathbf{k}}$ matrix. As a result, if $\mathcal{BR}_{\tilde{L}} \subset \mathcal{BR}_L$, the BCL flat band(s) satisfy the compatibility relations (as they must as linear combinations of band representations)[35,36] and carry bona fide (co)representations at all momenta, being generically gapped. Moreover, as gapped BCL flat bands are differences of band representations, they form a perfect playground for realizing fragile topological phases, which also emerge as differences of band representations[23,35,41–44].

On the other hand, if $\mathcal{BR}_{\tilde{L}}$ is not a subset of $\mathcal{BR}_L$ at some momentum point $\mathbf{K}$, then the flat bands are assigned a formal difference of (co)representations (for example, $\Xi \boxminus \Theta$) and must be degenerate with dispersive bands at $\mathbf{K}$. The corresponding band touching point is locally stable and cannot be gapped by any symmetry-preserving perturbation to the inter-sublattice matrix (Methods). At $\mathbf{K}$, the band touching point is faithfully described only by the representation Ξ, but the complete formal difference $\Xi \boxminus \Theta$ is required to fully characterize the flat bands. To see this, consider two band touching points given by $\Xi \boxminus \Theta_1$ and $\Xi \boxminus \Theta_2$. To produce gapped flat bands in the two BCLs, different orbitals will need to be added in the L lattice (that is, orbitals that induce the Θ_1 and Θ_2 (co)irreps, respectively). Moreover, in the vicinity of $\mathbf{K}$, Θ_1 and Θ_2 will subduce to potentially different (co)irreps of the corresponding little group, effectively resulting in different (co)irreps being assigned to the flat bands.

To illustrate the band representation subtraction from equation (4), Fig. 1 presents two generalized BCL examples on the two-dimensional hexagonal lattice in the *P6/mmm*1′ group (Shubnikov space group 191.234 in the notation of the Bilbao Crystallographic Server)[35,36,45–47]. In both examples, the L sublattice contains *s* orbitals at the 3f Wyckoff position. In Fig. 1a, we place *s* orbitals at the 1a position in $\tilde{L}$, resulting in two degenerate flat bands with

$$\mathcal{B}_{\mathrm{FB}} = (\mathrm{A_g})_{3\mathrm{f}} \uparrow \mathcal{G} \boxminus \left(\mathrm{A_{1_g}}\right)_{3\mathrm{f}} \uparrow \mathcal{G} = \left(\Gamma_5^+\right) + (\mathrm{K_5}) + \left(\mathrm{M_3^-} \oplus \mathrm{M_4^-}\right),$$

as shown in Fig. 1b. Because all (co)irreps of $\mathcal{BR}_{\tilde{L}}$ are included in $\mathcal{BR}_L$, the flat bands are gapped. On the other hand, if $\tilde{L}$ contains *s* orbitals at the 2c position (as shown in Fig. 1c), $\mathcal{B}_{\mathrm{FB}} = (\mathrm{A_g})_{3\mathrm{f}} \uparrow \mathcal{G} \boxminus (\mathrm{A'_1})_{2\mathrm{c}} \uparrow \mathcal{G} = \left(\Gamma_5^+ \boxminus \Gamma_4^-\right) + (\mathrm{K_1}) + \left(\mathrm{M_3^-}\right)$ contains a formal (co)irrep difference at the Γ point, signalling the presence of a band touching point, as seen in Fig. 1d.

We conclude that $\mathcal{B}_{\mathrm{FB}}$ contains all the information about the locally stable band touching points protected by crystalline symmetries, some of which were only partially understood in terms of ad hoc counting rules of real-space eigenstates with finite support[22,40]. At a given momentum point $\mathbf{K}$, there are locally stable band touching points if the band representation subtraction results in a formal (co)irrep difference. On the other hand, if the subtraction rule in equation (4) generates direct sums of (co)irreps, the flat bands can always be locally gapped at $\mathbf{K}$. Note, however, that this does not preclude globally stable band touching points between the flat and dispersive bands (as shown in the example constructed in Supplementary Section IIE). A globally stable band touching point cannot be gapped completely by any symmetry-preserving perturbation to $S_{\mathbf{k}}$, but its location in the Brillouin zone can be changed.

Classification. Equation (4) shows that the (co)irreps of the BCL flat band and corresponding band touching points depend exclusively on the orbital content of the two sublattices. The flat-band (co)irreps ($\mathcal{B}_{\mathrm{FB}}$) are linear combinations of elementary band representations, with positive or negative integer coefficients (Methods), depending on whether the corresponding orbitals belong to L or $\tilde{L}$,

respectively. This allows us to leverage MTQC for classifying flat bands[35,36]. In addition, equation (4) hints that, whilst the set of all possible perfectly flat bands for a given Shubnikov space group $\mathcal{G}$ ($\mathcal{F}_\mathcal{G}$) is infinite, it is also finitely generated.

To obtain $\mathcal{F}_\mathcal{G}$ explicitly, we introduce a $(d_\mathcal{G}+1)$-dimensional symmetry data vector $\overline{B}$, where $d_\mathcal{G}$ is the total number of (co)irreps of $\mathcal{G}$ for all high-symmetry momenta (Methods). The first component of $\overline{B}$ is a positive entry specifying the number of flat bands indexed by $\mathcal{B}_{\mathrm{FB}}$, whilst the next $d_\mathcal{G}$ components specify the multiplicities of the flat-band (co)irreps. Because $\mathcal{B}_{\mathcal{FB}}$ can contain formal differences of (co)irreps (corresponding to gapless flat bands), the last $d_\mathcal{G}$ components of $\overline{B}$ can be negative. In Supplementary Section IIIB, we show that

$$\mathcal{F}_\mathcal{G} = \left\{ \overline{B} \in \mathbb{Z}^{d_\mathcal{G}+1} | \overline{B} = \sum_{i=1}^{r} p_i e_i, p_i \in \mathbb{Z}, p_1 > 0 \right\}, \qquad (5)$$

where r is the number of linearly independent elementary band representations in the Shubnikov space group $\mathcal{G}$, and e_i $(1 \le i \le r)$ is a set of integer $(d_\mathcal{G}+1)$-dimensional vectors which we term the flat-band bases. In Supplementary Section IIIH, we tabulate the flat-band bases for all 1,651 Shubnikov space groups, with or without spin–orbit coupling. This result is comprehensive over all symmetry groups and will be an invaluable tool in the experimental search for topological flat bands[34].

The space of gapped flat bands $\mathcal{F}_\mathcal{G}^{\mathrm{G}}$ is computed by restricting to those elements of $\mathcal{F}_\mathcal{G}$ with only non-negative entries, such that the flat bands carry a bona fide (co)representation at all momenta. Using techniques of polyhedral computation first introduced to band theory by ref. [43], we show explicitly that $\mathcal{F}_\mathcal{G}^{\mathrm{G}}$ is also finitely generated and derive an algorithm for computing the corresponding bases in Supplementary Section IIIC. Moreover, as differences of band representations, we show in Supplementary Section IIIE that gapped BCL flat bands can also realize any topologically fragile bands[23,35,41–44], making them an ideal playground for strongly correlated phases of matter. In Supplementary Section IIIF, we present a simple example illustrating the relation between gapped, gapless and topologically trivial bands.

Discussion

We have presented a general technique for designing crystalline systems with perfectly flat bands. Unlike previous flat-band models, our method can be applied to systems with any orbital content, spin–orbit coupling, and within any symmetry group. In particular, being less restrictive than the well-known line-graph construction, our procedure offers great hope for obtaining materials with flat bands near the Fermi energy, which realize exotic phases of matter. Reference [34] highlights six prototypical compounds hosting flat bands (among many others) which can be explained with our formalism.

Within the framework of MTQC, the BCL flat bands can be understood as formal differences of band representations. This connection allow us to obtain criteria for identifying locally stable band touching points between the flat and dispersive bands. In addition, we have shown that gapped BCL flat bands can realize any topologically fragile phase. Moreover, using the recently tabulated elementary band representations for all 1,651 Shubnikov space groups, we have constructed all possible symmetry data vectors that can be realized in flat bands, showing that the set is infinite, but finitely generated, and tabulating the corresponding bases. Our work has great implications for the study of flat bands. For example, our band touching point construction yields a host of new semi-metallic flat-band systems which, when gapped, can lead to new exotic phases of matter[24].

Online content

Any methods, additional references, Nature Research reporting summaries, source data, extended data, supplementary information, acknowledgements, peer review information; details of author contributions and competing interests; and statements of data and code availability are available at https://doi.org/10.1038/s41567-021-01445-3.

Received: 8 June 2021; Accepted: 1 November 2021;
Published online: 23 December 2021

References

1. Bistritzer, R. & MacDonald, A. H. Moiré bands in twisted double-layer graphene. *Proc. Natl Acad. Sci. USA* **108**, 12233–12237 (2011).
2. Cao, Y. et al. Correlated insulator behaviour at half-filling in magic-angle graphene superlattices. *Nature* **556**, 80–84 (2018).
3. Cao, Y. et al. Unconventional superconductivity in magic-angle graphene superlattices. *Nature* **556**, 43–50 (2018).
4. Po, H. C., Zou, L., Vishwanath, A. & Senthil, T. Origin of mott insulating behavior and superconductivity in twisted bilayer graphene. *Phys. Rev. X* **8**, 031089 (2018).
5. Po, H. C., Zou, L., Senthil, T. & Vishwanath, A. Faithful tight-binding models and fragile topology of magic-angle bilayer graphene. *Phys. Rev. B* **99**, 195455 (2019).
6. Song, Z. et al. All magic angles in twisted bilayer graphene are topological. *Phys. Rev. Lett.* **123**, 036401 (2019).
7. Xie, F., Song, Z., Lian, B. & Bernevig, B. A. Topology-bounded superfluid weight in twisted bilayer graphene. *Phys. Rev. Lett.* **124**, 167002 (2020).
8. Mielke, A. Ferromagnetic ground states for the Hubbard model on line graphs. *J. Phys. A* **24**, L73–L77 (1991).
9. Mielke, A. & Tasaki, H. Ferromagnetism in the Hubbard model. *Commun. Math. Phys.* **158**, 341–371 (1993).
10. Wu, C., Bergman, D., Balents, L. & Das Sarma, S. Flat bands and Wigner crystallization in the honeycomb optical lattice. *Phys. Rev. Lett.* **99**, 070401 (2007).
11. Huber, S. D. & Altman, E. Bose condensation in flat bands. *Phys. Rev. B* **82**, 184502 (2010).
12. Goda, M., Nishino, S. & Matsuda, H. Inverse Anderson transition caused by flatbands. *Phys. Rev. Lett.* **96**, 126401 (2006).
13. Chalker, J. T., Pickles, T. S. & Shukla, P. Anderson localization in tight-binding models with flat bands. *Phys. Rev. B* **82**, 104209 (2010).
14. Mielke, A. Ferromagnetism in the Hubbard model on line graphs and further considerations. *J. Phys. A* **24**, 3311–3321 (1991).
15. Mielke, A. Exact ground states for the Hubbard model on the Kagome lattice. *J. Phys. A* **25**, 4335–4345 (1992).
16. Mielke, A. Exact results for the U = infinity Hubbard model. *J. Phys. A* **25**, 6507–6515 (1992).
17. Huda, M. N., Kezilebieke, S. & Liljeroth, P. Designer flat bands in quasi-one-dimensional atomic lattices. *Phys. Rev. Res.* **2**, 043426 (2020).
18. Liu, H. et al. Observation of flat bands due to band hybridization in the 3d-electron heavy-fermion compound $CaCu_3Ru_4O_{12}$. *Phys. Rev. B* **102**, 035111 (2020).
19. Meier, W. R. et al. Flat bands in the CoSn-type compounds. *Phys. Rev. B* **102**, 075148 (2020).
20. Baboux, F. et al. Bosonic condensation and disorder-induced localization in a flat band. *Phys. Rev. Lett.* **116**, 066402 (2016).
21. Kollár, A. J., Fitzpatrick, M. & Houck, A. A. Hyperbolic lattices in circuit quantum electrodynamics. *Nature* **571**, 45–50 (2019).
22. Bergman, D. L., Wu, C. & Balents, L. Band touching from real-space topology in frustrated hopping models. *Phys. Rev. B* **78**, 125104 (2008).
23. Chiu, C. S., Ma, D.-S., Song, Z.-D., Bernevig, B. A. & Houck, A. A. Fragile topology in line-graph lattices with two, three, or four gapped flat bands. *Phys. Rev. Res.* **2**, 043414 (2020).
24. Ma, D.-S. et al. Spin-orbit-induced topological flat bands in line and split graphs of bipartite lattices. *Phys. Rev. Lett.* **125**, 266403 (2020).
25. Lieb, E. H. Two theorems on the Hubbard model. *Phys. Rev. Lett.* **62**, 1201–1204 (1989).
26. Weaire, D. & Thorpe, M. F. Electronic properties of an amorphous solid. I. a simple tight-binding theory. *Phys. Rev. B* **4**, 2508–2520 (1971).
27. Tasaki, H. Ferromagnetism in the Hubbard models with degenerate single-electron ground states. *Phys. Rev. Lett.* **69**, 1608–1611 (1992).
28. Green, D., Santos, L. & Chamon, C. Isolated flat bands and spin-1 conical bands in two-dimensional lattices. *Phys. Rev. B* **82**, 075104 (2010).
29. Hatsugai, Y. & Maruyama, I. Z_Q topological invariants for polyacetylene, kagome and pyrochlore lattices. *Europhys. Lett.* **95**, 20003 (2011).

30. Raoux, A., Morigi, M., Fuchs, J.-N., Piéchon, F. & Montambaux, G. From dia- to paramagnetic orbital susceptibility of massless fermions. *Phys. Rev. Lett.* **112**, 026402 (2014).
31. Derzhko, O., Richter, J. & Maksymenko, M. Strongly correlated flat-band systems: the route from Heisenberg spins to Hubbard electrons. *Int. J. Mod. Phys. B* **29**, 1530007 (2015).
32. Leykam, D., Andreanov, A. & Flach, S. Artificial flat band systems: from lattice models to experiments. *Adv. Phys. X* **3**, 1473052 (2018).
33. Liu, H., Sethi, G., Meng, S. & Liu, F. Orbital design of flat bands in non-line-graph lattices via line-graph wavefunctions. Preprint at https://arxiv.org/abs/2104.14163 (2021).
34. Regnault, N. et al. Catalogue of flat band stoichiometric materials. Preprint at https://arxiv.org/abs/2106.05287 (2021).
35. Bradlyn, B. et al. Topological quantum chemistry. *Nature* **547**, 298–305 (2017).
36. Elcoro, L. et al. Magnetic topological quantum chemistry. *Nat. Commun.* **12**, 5965 (2021).
37. Kruthoff, J., de Boer, J., van Wezel, J., Kane, C. L. & Slager, R.-J. Topological classification of crystalline insulators through band structure combinatorics. *Phys. Rev. X* **7**, 041069 (2017).
38. Po, H. C., Vishwanath, A. & Watanabe, H. Symmetry-based indicators of band topology in the 230 space groups. *Nat. Commun.* **8**, 50 (2017).
39. Watanabe, H., Po, H. C. & Vishwanath, A. Structure and topology of band structures in the 1651 magnetic space groups. *Sci. Adv.* **4**, eaat8685 (2018).
40. Hwang, Y., Rhim, J.-W. & Yang, B.-J. Flat bands with band crossings enforced by symmetry representation. *Phys. Rev. B* **104**, L081104 (2021).
41. Cano, J. et al. Topology of disconnected elementary band representations. *Phys. Rev. Lett.* **120**, 266401 (2018).
42. Po, H. C., Watanabe, H. & Vishwanath, A. Fragile topology and wannier obstructions. *Phys. Rev. Lett.* **121**, 126402 (2018).
43. Song, Z.-D., Elcoro, L., Xu, Y.-F., Regnault, N. & Bernevig, B. A. Fragile phases as affine monoids: classification and material examples. *Phys. Rev. X* **10**, 031001 (2020).
44. Song, Z.-D., Elcoro, L. & Bernevig, B. A. Twisted bulk-boundary correspondence of fragile topology. *Science* **367**, 794–797 (2020).
45. Vergniory, M. G. et al. Graph theory data for topological quantum chemistry. *Phys. Rev. E* **96**, 023310 (2017).
46. Elcoro, L. et al. Double crystallographic groups and their representations on the Bilbao Crystallographic Server. *J. Appl. Crystallogr.* **50**, 1457–1477 (2017).
47. Xu, Y. et al. High-throughput calculations of magnetic topological materials. *Nature* **586**, 702–707 (2020).

Methods

The dispersive bands' (co)irreps of $T_{\mathbf{k}}$ and $\tilde{T}_{\mathbf{k}}$. At a high-symmetry momentum point $\mathbf{K}$, the first-quantized BCL Hamiltonian $H_{\mathbf{K}}$ must be invariant under the symmetry operations of $\mathcal{G}_{\mathbf{K}}$, the little group of $\mathbf{K}$. Since the sublattices obey the symmetries of $\mathcal{G}$ (which is a supergroup of $\mathcal{G}_{\mathbf{K}}$), every symmetry operation $g \in \mathcal{G}_{\mathbf{K}}$ is implemented individually in sublattice L ($\tilde{L}$) by a unitary matrix $U(g)$ [$\tilde{U}(g)$] such that $\hat{g}\hat{a}^{\dagger}_{i,\mathbf{K}}\hat{g}^{-1} = \sum_{j=1}^{N_L} U_{ji}(g)\hat{a}^{\dagger}_{j,\mathbf{K}}$ [$\hat{g}\hat{b}^{\dagger}_{i,\mathbf{K}}\hat{g}^{-1} = \sum_{j=1}^{N_{\tilde{L}}} \tilde{U}_{ji}(g)\hat{b}^{\dagger}_{j,\mathbf{K}}$]. Consequently (Supplementary Section IE), the inter-sublattice hopping matrix is invariant under the symmetry g, that is, $U(g)S^{(*)}_{\mathbf{K}}\tilde{U}^{\dagger}(g) = S_{\mathbf{K}}$, where $^{(*)}$ denotes complex conjugation when g is anti-unitary. Next, we consider two sets of eigenstates $\phi_{\mathbf{K},\beta}$ and $\psi_{\mathbf{K},\beta}$ (labelled by β) corresponding to the two effective Hamiltonians $T_{\mathbf{K}}$ and $\tilde{T}_{\mathbf{K}}$ with identical eigenvalues $\epsilon^2_{\mathbf{K},\beta} = \mathcal{E}^2$ (with $\mathcal{E} > 0$). Under the symmetry g, the eigenstates $\psi_{\mathbf{K},\beta}$ will transform under a certain (co)irrep $\mathcal{R}^{\mathcal{E}}_{\mathbf{K}}$ of the little group $\mathcal{G}_{\mathbf{K}}$, that is,

$$\tilde{U}(g)\psi^{(*)}_{\mathbf{K},\beta} = \sum_{\alpha}\left[\mathcal{R}^{\mathcal{E}}_{\mathbf{K}}(g)\right]_{\beta\alpha}\psi_{\mathbf{K},\alpha}, \tag{6}$$

where the sum runs over the states α for which $\epsilon_{\alpha,\mathbf{K}} = \mathcal{E}$. Left-multiplying equation (6) by $\frac{1}{\mathcal{E}}S_{\mathbf{K}}$ and employing the invariance of $S_{\mathbf{K}}$ under the group $\mathcal{G}_{\mathbf{K}}$ as well as the mapping between the nonzero eigenstates of $\tilde{T}_{\mathbf{K}}$ and $T_{\mathbf{K}}$, we find that

$$\frac{1}{\mathcal{E}}S_{\mathbf{K}}\tilde{U}(g)\psi^{(*)}_{\mathbf{K},\beta} = U(g)\phi^{(*)}_{\mathbf{K},\beta} = \sum_{\alpha}\left[\mathcal{R}^{\mathcal{E}}_{\mathbf{K}}(g)\right]_{\beta\alpha}\phi_{\mathbf{K},\alpha}. \tag{7}$$

Equation (7) implies that the set of eigenstates $\phi_{\mathbf{K},\beta}$ of the Hamiltonian $T_{\mathbf{K}}$ will transform according to the same (co)irrep $\mathcal{R}^{\mathcal{E}}_{\mathbf{K}}$ of the little group $\mathcal{G}_{\mathbf{K}}$ as $\psi_{\mathbf{K},\beta}$. As such, we find that the dispersive bands of $T_{\mathbf{k}}$ and $\tilde{T}_{\mathbf{k}}$ are not only identical in energies but also share the same (co)irreps.

Symmetry-enforced band touching points. Equation (4) provides a means of diagnosing the symmetry-enforced band touching points between the BCL flat and dispersive bands. Here, we show this by leveraging the fact that a generalized BCL from equation (3) with $A_{\mathbf{k}} = a\mathbb{1}$ and generic $B_{\mathbf{k}}$ shares the same flat-band (and corresponding band touching points) wavefunctions as $T_{\mathbf{k}}$. For a proof that does not rely on the effective Hamiltonians, see Supplementary Section IF.

Consider first the case when $\mathcal{BR}_{\tilde{L}}$ is contained within $\mathcal{BR}_L$ at a given momentum point $\mathbf{K}$, such that equation (4) results in a bona fide representation at $\mathbf{K}$. Now assume that the inter-sublattice hopping matrix is not full-rank at $\mathbf{K}$ (that is, $r_{\mathbf{K}} < N_{\tilde{L}}$), and thus that the flat bands of $T_{\mathbf{k}}$ are not gapped at $\mathbf{k}=\mathbf{K}$. The nonzero-energy eigenstates of $\tilde{T}_{\mathbf{K}}$ furnish the same (co)irreps of $\mathcal{G}_{\mathbf{K}}$ as the nonzero-energy eigenstates of $T_{\mathbf{K}}$. Because $\mathcal{BR}_{\tilde{L}}$ is a subset of $\mathcal{BR}_L$ at $\mathbf{K}$, it follows that, for any (co)irrep Ξ in the kernel of $\tilde{T}_{\mathbf{K}}$, there will be an identical (co)irrep Ξ in the kernel of $T_{\mathbf{K}}$. More precisely, let $\Xi \in \mathcal{BR}_{\tilde{L}}$ be a (co)irrep of $\mathcal{G}_{\mathbf{K}}$, whose carrier space is given by the states $\psi_{\mathbf{K},\beta}$, for which $\tilde{T}_{\mathbf{K}}\psi_{\mathbf{K},\beta} = 0$. The (co)irrep Ξ will also have a carrier space within the eigenstates belonging to the kernel of $T_{\mathbf{K}}$: $\phi_{\mathbf{K},\beta}$, with $T_{\mathbf{K}}\phi_{\mathbf{K},\beta}=0$. As $\psi_{\mathbf{K},\beta}$ and $\phi_{\mathbf{K},\beta}$ form carrier spaces for the same (co)irrep Ξ, the inter-sublattice hopping matrix can be perturbed without breaking any crystalline symmetries

$$S_{\mathbf{K}} \to S_{\mathbf{K}} + \mu\sum_{\beta}\phi_{\mathbf{K},\beta}\psi^{\dagger}_{\mathbf{K},\beta}, \tag{8}$$

resulting in $\phi_{\mathbf{K},\beta}$ and $\psi_{\mathbf{K},\beta}$ becoming eigenstates with eigenvalue $|\mu|^2$ of $T_{\mathbf{K}}$ and $\tilde{T}_{\mathbf{K}}$, respectively, and gapping the BCL flat bands at $\mathbf{K}$. Therefore, there can be no locally stable band touching points between the flat and dispersive BCL bands at some momentum $\mathbf{K}$, if $\mathcal{BR}_{\tilde{L}}$ is a subset of $\mathcal{BR}_L$ at $\mathbf{K}$.

On the other hand, if $\mathcal{BR}_{\tilde{L}}$ is not a subset of $\mathcal{BR}_L$ at momentum $\mathbf{K}$, the flat band is assigned the formal (co)irrep difference $\Xi \boxminus \Theta$, which cannot be simplified to a direct sum of (co)irreps. This means that the multiplicity of Ξ (Θ) in $\mathcal{BR}_L$ ($\mathcal{BR}_{\tilde{L}}$) is higher by one than in $\mathcal{BR}_{\tilde{L}}$ ($\mathcal{BR}_L$). Because of the one-to-one mapping of positive-energy eigenstates of the two effective Hamiltonians, it follows that the carrier space of Ξ (Θ) having dimension d_{Ξ} (d_{Θ}) is the kernel of $T_{\mathbf{K}}$ ($\tilde{T}_{\mathbf{K}}$), where $d_{\Xi} - d_{\Theta} = N_L - N_{\tilde{L}}$ (since $T_{\mathbf{K}}$ and $\tilde{T}_{\mathbf{K}}$ have the same rank). The kernel of $T_{\mathbf{K}}$ having dimension d_{Ξ} includes the $N_L - N_{\tilde{L}}$ flat-band eigenstates. Hence, the flat bands in $T_{\mathbf{K}}$ (and in the corresponding generalized BCL) will touch exactly d_{Θ} dispersive bands at $\mathbf{K}$. There is no symmetry-preserving perturbation that can be added to the inter-sublattice hopping matrix $S_{\mathbf{k}}$ to gap this band touching point. We thus conclude that it is locally stable and protected by the crystalline symmetries of $\mathcal{G}$.

Elementary band representations. The symmetry properties of an electronic band are completely described by its decomposition into (co)irreps at high-symmetry momenta in the Brillouin zone[35–39]. For a given gapped band or set of bands, the (co)irreps at two different momentum points are not independent, but instead have to satisfy certain compatibility relations[35–39,45,46]. The (co)irreps at the maximal momenta determine the (co)irreps across the entire Brillouin zone[35,36].

For any set of bands, we define an augmented symmetry data vector $\overline{B}$[35,36], which contains the multiplicities of all its (co)irreps at maximal momenta in the Brillouin zone (Supplementary Section IIIA,B)

$$\overline{B} = \begin{pmatrix} n \\ m\left(\rho^1_{\mathcal{G}_{\mathbf{K}_1}}\right) \\ m\left(\rho^2_{\mathcal{G}_{\mathbf{K}_1}}\right) \\ \vdots \\ m\left(\rho^1_{\mathcal{G}_{\mathbf{K}_2}}\right) \\ m\left(\rho^2_{\mathcal{G}_{\mathbf{K}_2}}\right) \\ \vdots \end{pmatrix}. \tag{9}$$

In equation (9), $m\left(\rho^i_{\mathcal{G}_{\mathbf{K}_j}}\right)$ denotes the multiplicity of the (co)irrep $\rho^i_{\mathcal{G}_{\mathbf{K}_j}}$ of the little group $\mathcal{G}_{\mathbf{K}_j}$ of the maximal momentum $\mathbf{K}_j$. Compared with an ordinary symmetry data vector[35,36], $\overline{B}$ contains one additional entry (n) at the beginning, specifying the number of bands encoded by $\overline{B}$. To restrict to physical flat-band systems, we enforce $n>0$, as a negative number of bands is unphysical.

A central role in MTQC is played by the elementary band representations. An elementary band representation is a special type of (atomic) (co)representation of the Shubnikov space group that is induced from a certain (co)irrep of the site-symmetry group of a maximal Wyckoff position[35,36]. The great power of MTQC stems from enumerating all possible elementary band representations within a given symmetry group. Since the (co)irreps of $\mathcal{BR}_L$ and $\mathcal{BR}_{\tilde{L}}$ are induced from atomic limits, the band representations are just linear combinations of elementary band representations. As a result of this and equation (4), the flat-band augmented symmetry data vectors are just linear combinations of elementary band representations. This implies that the set of all augmented symmetry data vectors corresponding to BCL flat bands can be written as equation (5) (Supplementary Section IIIB).

Data availability

All data related to this paper are available in the Supplementary Information.

Code availability

The code necessary to generate the flat-band bases can be made available upon request from the authors.

Acknowledgements

We thank M.-R. Li and D.-S. Ma for fruitful discussions and collaboration on related projects. This work is part of a project that has received funding from the European Research Council under the European Union's Horizon 2020 research and innovation programme (grant agreement no. 101020833). B.A.B. and N.R. were also supported by the US Department of Energy (grant no. DE-SC0016239), and were partially supported by the National Science Foundation (EAGER grant no. DMR 1643312), a Simons Investigator grant (no. 404513), the Office of Naval Research (ONR grant no. N00014-20-1-2303), the Packard Foundation, the Schmidt Fund for Innovative Research, the BSF Israel US foundation (grant no. 2018226), the Gordon and Betty Moore Foundation through grant no. GBMF8685 towards the Princeton theory programme and a Guggenheim Fellowship from the John Simon Guggenheim Memorial Foundation. B.A.B. and N.R. were supported by the NSF-MRSEC (grant bo. DMR-2011750). B.A.B. and N.R. gratefully acknowledge financial support from the Schmidt DataX Fund at Princeton University made possible through a major gift from the Schmidt Futures Foundation. L.E. was supported by the Government of the Basque Country (project IT1301-19) and the Spanish Ministry of Science and Innovation (PID2019-106644GB-I00). Further support was provided by the NSF-MRSEC no. DMR-1420541, BSF Israel US Foundation no. 2018226 and the Princeton Global Network Funds.

Author contributions

D.C., A.C., L.E. and B.A.B. conceived the work and the main idea of band representation subtraction. D.C., A.C., Z.-D.S., L.E. and B.A.B. contributed to the theory of generalized BCL construction, band representation subtraction and gapless point criteria. D.C. and A.C. analysed the two-dimensional examples of flat-band constructions from Supplementary Section II, with input from Z.-D.S. and L.E. Y.X. performed the first-principles calculations from Supplementary Section IID, and analysed the flat-band crystalline material $Ca_2Ta_2O_7$. D.C., A.C., L.E. and Z.-D.S. performed the flat-band classification and compiled the tables. All authors discussed the results and wrote the main text and Methods. D.C. and A.C. wrote the Supplementary Information, with input and feedback from L.E., Z.-D.S., N.R., B.A.B. and Y.X.

Competing interests

The authors declare no competing interests.

Additional information

Supplementary information The online version contains supplementary material available at https://doi.org/10.1038/s41567-021-01445-3.

Correspondence and requests for materials should be addressed to B. Andrei Bernevig.

Peer review information *Nature Physics* thanks David Carpentier and the other, anonymous, reviewer(s) for their contribution to the peer review of this work.